Surface Acoustic Waves Grant Superior Spatial Control of Cells Embedded in Hydrogel Fibers

*James P. Lata, Feng Guo, Jinshan Guo, Po-Hsun Huang, Jian Yang, and Tony Jun Huang**

For many tissues, including bone, cardiac muscle, pancreas, and nerves, the arrangement of cells are required to enhance cell–cell communications and cell-extracellular matrix interactions which is of critical importance for tissue development and function.[1] These tissues have a high degree of cellular architecture which is created with repeating units of similar cells to allow efficient communication in a synergistic manner to perform a given function.[2] For example, nerve tissue contains neurons located at specific locations with synaptic linkages for long-distance communications, whereas muscle tissues comprise many cells in close proximity in a fiber formation to carry out contractile motions.[3] Thus, being able to pattern cells to mimic these different cellular architectures will yield more physiological tissue functions for tissue engineering compared to seeding or printing cells without a predefined pattern.

Tissue engineering primarily focuses on developing materials which stimulate cell growth and rely on cell self-assembly to build functional tissues, however little attention is focused on the organization of the seeded cells. For most widely used tissue engineering strategies, cells are seeded on top of scaffolding materials, or decellularized tissue-derived scaffolds,[4] where they attach and proliferate in more or less a 2D plane along the scaffold. To better capitulate the native tissue and have a better control on 3D scaffolding, current methods have shifted toward 3D bioprinting where cells are seeded or encased into the scaffold material itself, allowing for proliferation and cell–cell contacts in a 3D manner.[5] Embedding cells into materials with low biodegradability also protects the cells from being rejected by the host's immune system.[6] 3D bioprinting of cells within a polymer solution have great advantages for large-scale organ construction, however cellular organization is not taken into account which could lead to inefficient or failed overall function of these printed tissues. While there are many other types of encapsulation techniques, novel materials, and processes for manipulating the geometry of these materials,[6,7] the organization of the cells within these materials is very much lacking.

Dr. J. P. Lata, Dr. F. Guo, Dr. P.-H. Huang, Prof. T. J. Huang
Department of Engineering Science and Mechanics
The Pennsylvania State University
University Park, PA 16802, USA
E-mail: junhuang@engr.psu.edu
Dr. J. Guo, Prof. J. Yang
Department of Biomedical Engineering
The Pennsylvania State University
University Park, PA 16802, USA

DOI: 10.1002/adma.201602947

Tools thus far used to pattern cells within, or on top of, scaffolds have utilized optical forces, magnetic forces, hydrodynamic forces, dielectrophoretic forces, biomolecular/chemical coatings, or alterations of substrate pattern, geometry, and porosity.[8] One of the most promising innovations for cellular control in a scaffold environment is through microfluidic coaxial flow. This method controls the flow characteristics of a polymer solution, usually alginate with extracellular matrix (ECM) proteins, and has the ability to code different cell types within a single 200 μm fiber.[9] However, the spatial control of cells is poor. This strategy cannot control the distribution of individual cells or clusters of cells within the fiber, relying on simple microfluidic flow to position regions of disorganized cells either parallel to one another or in a repeating sequence along the fiber. There does not exist a method which can easily make repeat unit patterns of cells while controlling cellular distance. This precise control of the cellular architecture needs to be achieved in order to truly recapitulate a tissues function.

A promising way to manipulate individual cells or clusters of cells in a noninvasive, biocompatible, contactless, and label-free manner is through surface acoustic waves (SAWs).[10] We have demonstrated the unique capabilities of SAW to massively pattern cells in a 3D manner within a phosphate buffered saline (PBS) buffer or cell media environment while maintaining high spatial resolution.[11] The SAW-based patterned cells displayed normal morphological spreading after dropping to the surface. This type of patterning mimics physiological patterns found in tissues by producing repeating cellular units with precise spacing between them. Many tissues utilize these repeating cellular units to carry out synergistic tasks, which require a great number of like cells to work in unison, such as muscle contraction in muscle tissue, signal propagation in neuronal tissue, or toxin processing in liver tissue.[12] Thus the spacing or configuration of cells is very important to achieve physiologically relevant tissue function.

In view of the SAW patterning capabilities, we take this technology a step further to use in tissue engineering applications by arranging cells within a viscous polymer medium to create cellular fibers with defined patterns which can be used to build complex 3D tissue architectures. SAWs have thus far been used solely for lab-on-a-chip processes, where everything is designed to be utilized in the microfluidic chamber. This will be the first time we separate from on-chip designs and utilize the structures built by SAWs outside of the chip environment. We chose a fiber geometry, as opposed to sheets, as it is more durable and easy to manipulate. Fibers can also be built into complex 3D structures with varying cell types, yielding excellent diffusion characteristics due to the large pore sizes

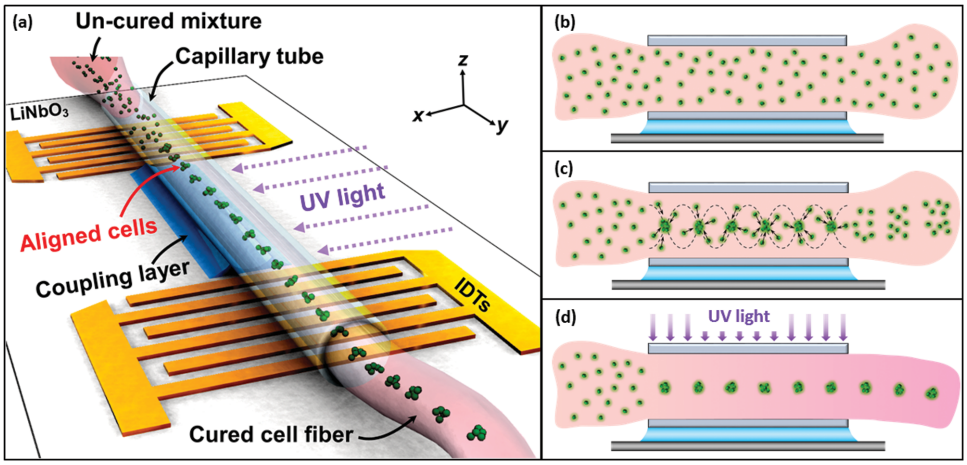

Scheme 1. a) Schematic representation of the entire process for generating a patterned cell fiber in the perpendicular orientation using SAWs. b) The photosensitive polymer and cell solution is added to a tube which is atop a piezoelectric substrate containing two parallel IDTs with a water-coupling layer. c) IDTs are activated which produce SAWs that align the cells. d) Following IDT deactivation, the fiber is polymerized with UV light and extracted, retaining cell patterns.

between the fibers.[6,13] Our method for creating these fibers can utilize a variety of photosensitive polymers which can be robust and tuned for biodegradability.[14] Here, we demonstrate the patterning of HeLa cells in poly(ethylene glycol) diacrylate (PEGDA) and methacrylated gelatin (GelMA)[15] solutions, and confirm high cell viability after fiber extraction.

In this work, we used a piezoelectric substrate ($LiNbO_3$) deposited with a pair of parallel interdigital transducers (IDTs). Between the IDTs we placed a water coupling layer onto the piezoelectric substrate which was used to guide the propagation of leaky waves from the substrate into the tube superstrate above. **Scheme 1** shows the experimental apparatus and the entire process for creating embedded cell fibers with predefined cellular patterns. The two main superstrates were 100 µm inside diameter (ID)/200 µm outside diameter (OD) square bore glass capillary tubes and 280 µm ID/610 µm OD polyethylene tubing. Microbeads or HeLa cells were mixed within polymer solutions containing either 10% PEGDA 700, 10% PEGDA 3400, or a combination of 10% PEGDA 3400 with 2% GelMA, as well as Irgacure 2959 photoinitiator and pluronic F-127. Each of these polymer solutions was tested with the SAW device for the ability to align objects, polymerize the polymer, and extract the aligned fiber. Last, the fibers were manually manipulated to create simple architectures, where cell fibers are placed next to one another in rows, and complex architectures, where cell fibers are woven together in a weave formation, with emphasis on the cell alignment.

The alignment of objects (microbeads or cells) using a SAW device relies on the position of the object to the incident wave and the distribution of forces acting upon the object. For these experiments we either chose a perpendicular alignment, where the object is to be patterned perpendicular to the incident waves and thus the tube placed perpendicular to the IDTs, or a parallel alignment, where the object is to be patterned parallel to the incident wave having the tube positioned parallel to the IDTs. The force distribution on the object can be broken down into the acoustic radiation force, drag, and friction/wall effect forces,[16] streaming and buoyancy forces, and the gravitational force.[11d] In order for the object to be manipulated the acoustic force must surpass the balancing of all other forces. In this work we demonstrate how powerful SAWs can be, not only do they need to travel through a coupling layer into a superstrate but they have to manipulate objects which are in a highly viscous medium compared to water. This is of particular importance as viscous medium will cause an attenuation in the acoustic energy, making manipulation of objects more difficult.[17] We tested three polymers (PEGDA 700, PEGDA 3400, and GelMA) for their performance of acoustic manipulation within glass capillary tubes. These polymers were chosen based on their prior use in tissue engineering and embedded cell technologies.[18] With a given input power density (1.5 W cm^{-2}) and frequency (12.65 MHz) all three polymer solutions allowed SAWs to pattern both 10 µm beads as well as HeLa cells within the channel. Cells have many intrinsic characteristics which differ greatly from beads, such as rigidity, morphology, density, and acoustic impedance, which all affect SAW's performance. In this work, we demonstrate that our platform can effectively manipulate both beads and cells given the same SAW parameters. A representative polymer solution, PEGDA 700, is shown in **Figure 1** to demonstrate the patterning efficiency of both beads and HeLa cells in glass capillary tubes. We define patterning efficiency as the percentage of objects aligned at the SAW nodal positions. We assign excellent patterns as >80%, good patterns between 60%–80%, poor patterns between 30%–60%, and no pattern below 30%. In all our experiments, patterning efficiency was greater than 80% displaying excellent patterns. It is worth noting that it only takes seconds to achieve a very well-defined pattern as is shown in Videos S1 and S2 (Supporting Information). Being able to pattern within different photosensitive polymers with differing viscosities demonstrates the versatility of our technology, and therefore is not limited to a specific polymer.

To take the patterning a step further we decided to move away from glass capillary tubes and to a much more inexpensive and flexible material, polyethylene tubing. The plastic

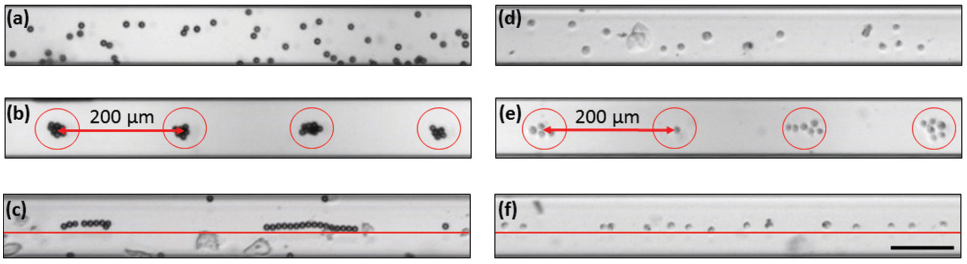

Figure 1. Patterning of micro-objects using SAWs within a viscous polymer solution (10% PEGDA 700) in a glass capillary tube. a–c) 10 μm beads or d–f) HeLa cells were placed into a,d) a tube and then patterned either b,e) perpendicular or c,f) parallel to the IDTs. Perpendicular alignment created repeating clusters of micro-objects at ½ SAW wavelength (400 μm), while parallel alignment created straight lines of micro-objects. Scale bar: 100 μm.

tubing greatly changes the vertical working distance of the SAWs. Its wall thickness and interior bore size are much larger than those of the glass capillaries, being more than three times thicker and almost three times the bore size. Manipulating objects from such a large vertical working distance and with a viscous medium has not been shown before using SAWs. However, we demonstrate that not only can we manipulate objects/cells but we can still obtain very well defined patterns along the entire IDT regime (≈1 cm) within the polyethylene tube as shown in Supplemental Video 3.

Once cells have the desired patterns, the IDTs are turned off and a UV light is applied for 30 s to polymerize the polymer solution. It has been shown that the photopolymerization process has minimal effects on embedded cells within hydrogel polymers.[14c] For these experiments, we used 10% PEGDA 3400 as it displayed a much higher cell viability postpolymerization compared to the 10% PEGDA 700. The polymerized fibers are extracted from the tubes by applying pressure with a syringe at one end. The fibers slide out smoothly from their encasement and are placed into Dulbecco's modified Eagle's medium (DMEM) for visualization and culture. The diameter of the extracted fiber is dependent on the bore size of the capillary used, thus these fibers are ≈280 μm in diameter.

Figure 2 displays aligned cells with short-term viability stain (explained below) inside a polyethylene tube after polymerization and extraction, with emphasis on the retention of the cell pattern. The pluronic aids in the extraction of the fibers by coating the tube, making it hydrophobic. If pluronic is not added to the polymer solution it will require a greater deal of strength to extract the PEGDA 700 and 3400 and make it nearly impossible to extract fibers with gelatin. While the tubes can be precoated with pluronic, having it in the polymer solution aids in cell viability.[19] Since the patterning was done while viewing the tubes in a 2D plane (on the microscope) we further investigated whether the cells were truly embedded within the fiber or were along the periphery of the fiber by rotating the extracted fiber, demonstrating the 3D encapsulation of the cells as shown in Video S4 (Supporting Information).

There were no limitations to the length of fiber as it is proportional to the length of tubing used. Here, we tested 1 to 6 cm fibers and had no difficulty with the polymerization or extraction, with longer fibers likely producible. In longer fibers (>3 cm) we can pattern different regions of the fiber, displaying regions where there are organized cells abutted to unorganized cells as shown in Figure S1 (Supporting Information), which is of particular interest in cellular communication and cell/tissue organization research.[20] Last, we show in Figure S2 (Supporting Information) that the alignment is not completely cell type dependent and that we can pattern different cell types such as MC3T3-E1 cells (an osteoblast precursor cell line for bone) and P12 Adh cells (a pheochromocytoma cell line which is similar to neuronal cells). Our results are promising for future studies that use these types of cells to take advantage of the cellular organization.

This entire fiber creation process contains multiple steps at which cell viability needed to be verified. To validate that cell viability was not dramatically impacted by our methodology, we performed short-term (<1 h) and long-term viability tests (2–10 h). Both tests utilized final concentrations of 1×10^{-6} M propidium iodide (PI) and calcein AM to stain for dead and live cells, respectively. Viability was calculated by counting the number of live cells and comparing with the number of dead cells, if any cells displayed PI stain it was counted as dead. Short-term staining took place within the initial polymer solution, before capillary injection, and cell viability was tracked from injecting the solution into the tube, through SAW alignment, UV polymerization, and right after extraction of the fiber.

Figure 2 shows fluorescent imaging of the cells with short-term viability stain after polymerization and fiber extraction, yielding ≈100% viability. Both SAW alignment and UV polymerization displayed no effect on cell viability. SAW and UV exposure time was tested up to 5 min with good viability results, however with 5 min of UV polymerization you can see ripples and stretch marks in the polymer, which will result in cell death. We also tested the irradiation and SAW exposure for 20 min as an extreme on the cells without polymer solution to validate that the UV and SAW had no effect upon the cells' short-term viability. In all cases, cells were almost 100% viable throughout the process.

Long-term viability did not use any stain in the original polymer solution. Instead fibers were patterned and extracted, then placed into media containing the viability stain. Each fiber was imaged every half hour within a culture chamber placed on the microscope stage. Setting up the chambers containing fibers takes about 1 h, and another hour is given to allow the viability stain to penetrate the polymer and cell fibers, thus we start looking at long-term viability at the 2 h time point. **Figure 3** contains bright-field and fluorescent viability stain images at 2, 5, and 10 h post-fiber extraction. Cells survived up to 10 h with negligible death (>90% cell viability). Figure S3 (Supporting Information) displays a control for UV exposure on cells with

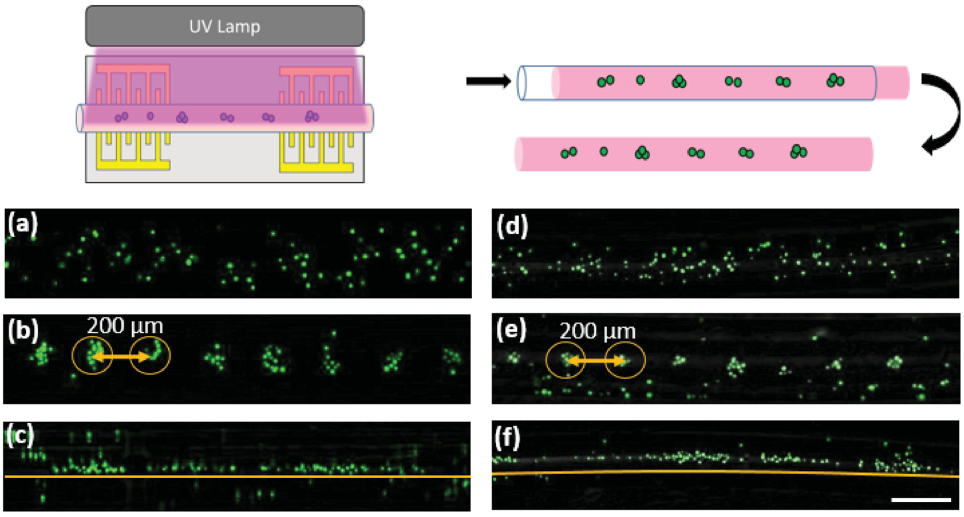

Figure 2. Polymerization and extraction of aligned cell fibers (10% PEGDA 3400) within a polyethylene tube, as well as short-term viability of cells via fluorescent imaging. a,d) Control fibers did not use SAW excitation and therefore have no alignment, compared to b,e) the perpendicular and c,f) parallel aligned cells by SAWs. Cell fibers are shown to undergo polymerization via a–c) UV irradiation and d–f) extraction [schematics displayed above to aid in understanding] without any adverse short-term viability effects on the cells (≈100% survival). Green stain represents live cells while red stain represents dead cells. Scale bar: 200 μm.

and without polymer solution after 24 h of culture, verifying that UV exposure did not result in dramatic cell death.

Once the patterned cell fibers were created, we assembled them into simple and complex architectures to demonstrate how the patterning of the cells affects the tissue layout, as well as aiding to conceptualize different cell types for each pattern. HeLa cells were stained with Cell Tracker Orange or Green to simulate two different cell types. All the cell fibers were manually assembled in cell culture medium and were attached through simple superposition. For the simple architecture, multiple long fibers aligned parallel or perpendicular were placed in rows as shown in **Figure 4**a, with a parallel fiber in the middle of two perpendicular fibers. For this architecture one can imagine the perpendicular fibers being muscle cells with the parallel fiber being nerve or vascular cells. Other variations of these rows, such as with four fibers and double fibers (2 aligned fibers per single fiber) are shown in Figure S4 (Supporting Information). The other architecture

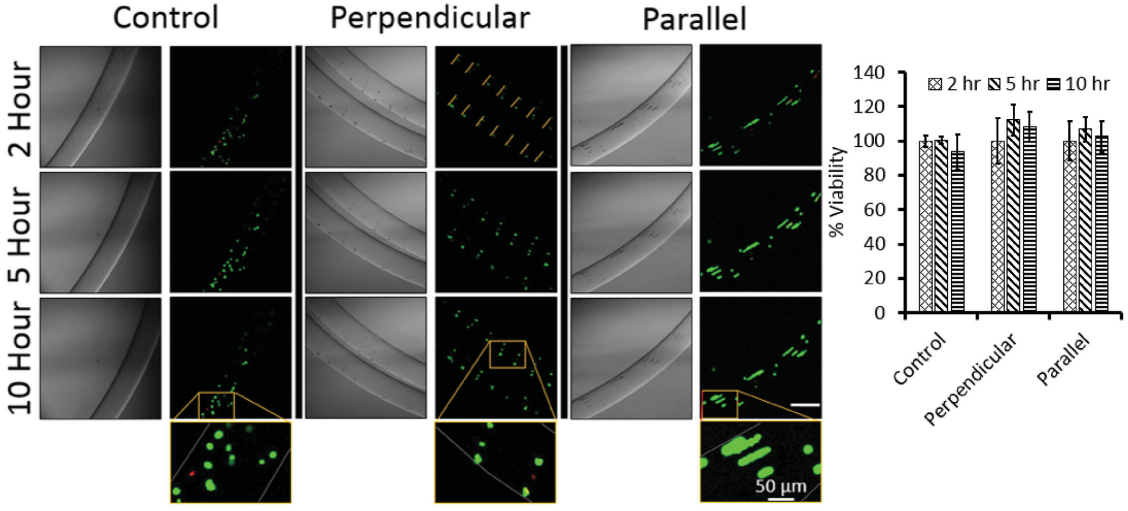

Figure 3. Long-term cell viability of control and SAW-aligned cellular fibers out to 10 h. After extraction, cell fibers were placed into DMEM media with viability stain and imaged every 30 min. Fluorescent images display the 2, 5, and 10 h time points for control fibers (without SAW) and cells aligned perpendicular and parallel to IDTs by SAWs. Green stain is used to visualize living cells while red stain is used to show dead cells. Yellow lines are added to guide the eye to perpendicular pattern. Magnifications are displayed for better visualization of the patterned cells. Bright-field images are added to display any movements of the fiber. The bar graph displays the percent cell viability starting from the 2 h time point out to 10 h. Each point represents at least four different fibers. The slight increase in cell viability at the 5 h time point is due to the viability stain reaching peak concentrations within the fiber. As shown, there is no statistical difference ($p > 0.1$) between the control and aligned fibers with negligible cell death throughout 10 h ($p > 0.1$). Scale bar: 200 μm.

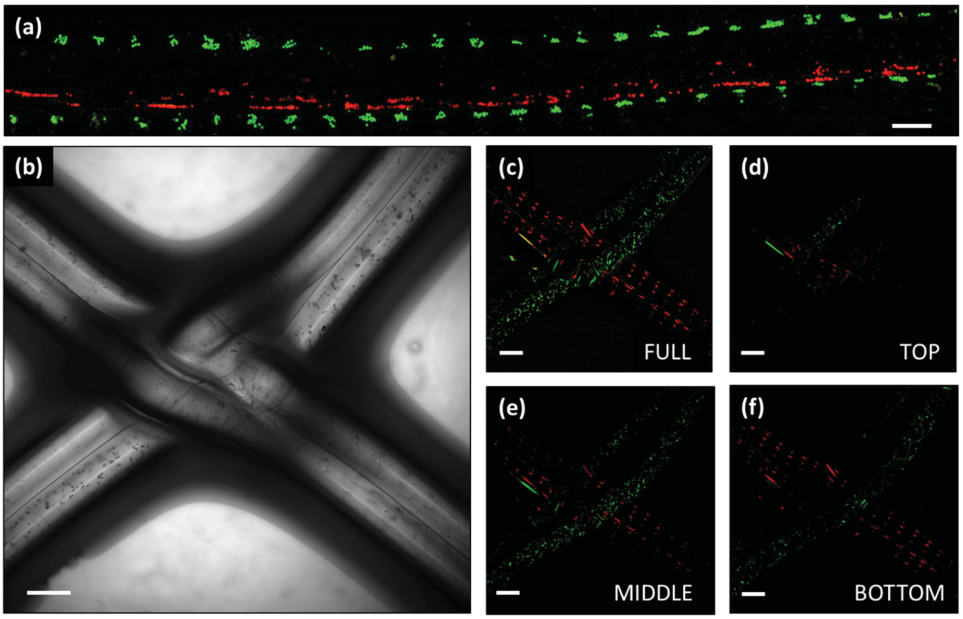

Figure 4. Simple and complex architecture were formed with patterned cell fibers. HeLa cells were incubated with Orange or Green Cell Tracker stain before patterning, to conceptualize multiple cell types. Cell fibers were then patterned, polymerized, and extracted. a) Long patterned fibers were placed in a row architecture with perpendicular patterned fibers (green) on the top and bottom and a parallel patterned fiber (red) in the middle. Complex architectures were also realized by manually weaving patterned fibers (red) into nonpatterned fibers (green) yielding a 2×2 weave architecture. b) A bright-field image displays the weave architecture while c) the fluorescent images display a full Z stack of the weave, as well as d) the top, e) middle, and f) bottom of the weave. Being able to manipulate the patterned fibers into complex architectures allows the creation of biomimetic cell alignment in tissues. Scale bars: 200 μm.

is more complex, making a weave with the fibers of different patterns. Figure 4b–f displays a 2×2 weave, where 2 perpendicular fibers are woven into 2 random fibers. This juxtaposition of the patterned versus nonpatterned fibers highlights the repeating cellular units found in physiological tissues, such as muscle, against what is typically used without cellular spatial control. Another example of the weave architecture is given in Figure S5 (Supporting Information), where parallel and perpendicular fibers are weaved in a 1×2 double fiber weave, utilizing 6 aligned fibers where 2 aligned fibers make up a single fiber. Both weave architectures were visualized through their Z stacks to show the 3D architecture in Videos S5–S8 (Supporting Information). More complex weave patterns can be performed with a greater number of fibers, however this would be more suited for a microfluidic handling platform as described in prior literature.[9]

In conclusion, we have developed a technique which can control the spatial distribution of cells and objects within photosensitive hydrogel fibers for use as a functional material in tissue engineering and cellular biology research. The power of SAWs was demonstrated by patterning particles and cells within highly viscous solutions and through thick plastic tubing walls, allowing for an inexpensive and reusable technology for disposable superstrate devices. Patterning was accomplished with different tubing materials and hydrogel matrices, demonstrating the versatility of the technology to fit different application parameters. The polymer solutions were polymerized using UV light and extracted with cell patterns preserved throughout the procedure. The entire process was proven safe for the cells as there was no loss in short-term viability. Long-term viability displayed over 90% of viable cells out to 10 h in culture conditions. Last, patterned fibers were manually manipulated into simple and complex architectures, demonstrating how the patterns could be used with different cell types to mimic different physiological tissues. We believe this technology to be paramount for tissue engineering applications which need to take into consideration the 3D cellular architecture, as well as biological research involving cell–cell communication and organization.

Experimental Section

Polymer Solution: Cultured HeLa S3 [CCL-2.2] cells (ATCC, USA), MC3T3-E1 [CRL-2593] cells (ATCC, USA), and PC12 Adh [CRL 1721.1] cells (ATCC, USA) were harvested separately with 0.05% trypsin and 0.53×10^{-3} M ethylenediaminetetraacetic acid (EDTA) solution (Corning, USA). The cells were washed and resuspended in warm DMEM (ATCC, USA) with 10% fetal bovine serum and 1% penicillin to an approximate concentration of 5×10^6 cells mL^{-1}. The polymers were diluted in DMEM to the following final concentrations (w/v) for each respective fiber: 10% PEGDA 700 (Sigma, USA), 10% PEGDA 3400 (Alfa Aesar, USA), and 10% PEGDA 3400 with 2% GelMA.[15a] Pluronic F-127 (Sigma, USA) was added to the polymers to a final concentration of 0.2% w/v in order to aid in cured polymer extraction as well as increased cell viability. Irgacure 2959 (Ciba Specialty Chemicals) photoinitiator was added at a final concentration of 0.05% and the solution was vortexed and warmed to 37 °C. Last, 10 μm poly(styrene/divinylbenzene) beads (Bangs Laboratory) or cells were added at 0.5% or 40% ($\approx 2 \times 10^6$ cells mL^{-1}) v/v final concentrations, respectively, and gently mixed by hand.

SAW Apparatus: The SAW device contained a 128° Y-cut lithium niobate ($LiNbO_3$) substrate (500 μm thick) and two chrome and gold (Cr/Au, 50 Å/500 Å) IDTs. The IDTs have a period of 400 μm which were

patterned through e-beam evaporation and a lift-off process.[21] The polymer solution was placed into either a glass, square bore, capillary tube (100 μm ID/200 μm OD, VitroTubes) through capillary force or a polyethylene fine bore Portex tube (280 μm/610 μm, Smiths Medical) with a 30G needle and syringe. A coupling liquid was placed between the tube and the piezoelectric substrate and between the two IDTs. A variety of coupling liquids (oil, water, UV epoxy) were assessed for their acoustic impedance, and while having a high evaporation rate (2–3 min), water demonstrated the best performance. The SAW device was mounted on the stage of an inverted microscope (TE2000U, Nikon, USA) and images were taken with a CCD camera (CoolSNAP HQ2, Photometrics, USA).

To align the beads or cells, both IDTs were connected to a function generator (AFG3102C, Tektronix, USA) and the radio frequency signals amplified with an amplifier (25A100A, Amplifier Research, USA). The input power density was 1.5 W cm^{-2} and the frequency was adjusted to 12.65 MHz to produce stable standing waves (λ = 400 μm). The tube with polymer solution was either placed perpendicular or parallel to the IDTs to yield a desired pattern. IDTs were activated for just 20 s to produce required alignment and then shut off. A 6 watt UV-AC hand lamp (VWR, USA) set to 254 nm wavelength was used for 30 s to cure the polymer solution within the tube. After polymerization a syringe was used to apply pressure to the newly formed fiber and the extracted fiber was placed into a Lab-Tek 16-well chamber slide (Thermo Fisher Scientific, USA) with 200 μL DMEM.

Viability: Cell viability was measured before SAW exposure, after SAW exposure, after polymerization, after fiber extraction, and from 2–20 h following extraction. Viability was calculated by counting live and dead cells through the use of PI to stain for dead cells and calcein acetoxymethyl (AM) to stain for live cells. Cells were counted as dead if they showed any amount of PI stain, even if they also showed high calcein AM. A final concentration of 1×10^{-6} M PI (Sigma, USA) and calcein AM (Sigma, USA) was added to the polymer solution, before injection into the capillary, to verify short-term cell viability (before SAW exposure, after SAW exposure, after polymerization, and after fiber extraction). Long-term cell viability was measured by submerging extracted fibers into a PI and calcein AM solution diluted to 1×10^{-6} M with DMEM and culturing them in a stage top incubator (INUG2-TIZ, Tokai Hit) while imaging every 30 min for 20 h. Percent viability was calculated as (# live cells)/(# live cells + # dead cells), for long-term viability. Each time point was normalized to the 2 h time point to display viability after 2 h. ImageJ (NIH, USA) and Excel (Microsoft, USA) were used for image analysis and statistics for cell viability. Sterilization was taken into account during the entire process of cell fiber production. The fibers were produced on an ethanol sterilized microscope slide. All needles, forceps, and tubing were sterilized with 70% ethanol before use. The extracted fibers were then transferred to a sterile culture chamber slide in a biosafety cabinet and cultured in a presterilized stage incubator.

Fiber Architectures: Cells were incubated for 30 min at 37 °C with CellTracker Orange CMRA or Green CMFDA (Thermo Fisher Scientific, USA) at 8×10^{-6} M. The cells were mixed with polymer solution using 10% PEGDA 3400 and 2% GelMA. The cell solution was patterned, polymerized, and the resulting fiber extracted. The patterned fibers were then manipulated with a syringe, applying negative pressure to one end of the fiber to move. Architectures were created and imaged with Z stack images taken for the complex architectures.

Supporting Information

Supporting Information is available from the Wiley Online Library or from the author.

Acknowledgements

The authors gratefully acknowledge financial support from the National Institutes of Health (Grant Nos. R01 GM112048 and R33 EB019785), National Science Foundation (Grant Nos. IIP-1534645 and IDBR-1455658), and the Penn State Center for Nanoscale Science (MRSEC) under Grant DMR-1420620. Components of this work were conducted at the Penn State node of the NSF-funded National Nanotechnology Infrastructure Network (NNIN).

Received: June 3, 2016
Revised: July 18, 2016
Published online: August 29, 2016

[1] N. C. Rivron, J. Rouwkema, R. Truckenmüller, M. Karperien, J. De Boer, C. A. Van Blitterswijk, *Biomaterials* **2009**, *30*, 4851.
[2] A. J. Engler, P. O. Humbert, B. Wehrle-Haller, V. M. Weaver, *Science* **2009**, *324*, 5.
[3] K. S. Saladin, in *Human Anatomy*, Vol. *2* (Ed: C. H. Wheatley), McGraw-Hill, New York **2008**.
[4] M. E. Scarrit, *Front. Bioeng. Biotechnol.* **2015**, *3*, 1.
[5] a) N. A. Sears, P. S. Dhavalikar, D. Seshadri, E. Cosgriff-Hernandez, *Tissue Eng. Part B: Rev.* **2016**, *4*, 298; b) S. Hong, D. Sycks, H. F. Chan, S. Lin, G. P. Lopez, F. Guilak, K. W. Leong, X. Zhao, *Adv. Mater.* **2015**, *27*, 4035; c) A. Arslan-Yildiz, R. E. Assal, P. Chen, S. Guven, F. Inci, U. Demirci, *Biofabrication* **2016**, *8*, 014103.
[6] A. Kang, J. Park, J. Ju, G. S. Jeong, S.-H. Lee, *Biomaterials* **2014**, *35*, 2651.
[7] a) P. de Vos, H. A. Lazarjani, D. Poncelet, M. M. Faas, *Adv. Drug Delivery Rev.* **2014**, *67*, 15; b) C. M. Puleo, H.-C. Yeh, T.-H. Wang, *Tissue Eng.* **2007**, *13*, 2839.
[8] a) S. Yamamoto, M. Okochi, K. Jimbow, H. Honda, *Biotechnol. Bioprocess Eng.* **2015**, *20*, 488; b) D. R. Albrecht, G. H. Underhill, T. B. Wassermann, R. L. Sah, S. N. Bhatia, *Nat. Methods* **2006**, *3*, 369; c) P. Chen, Z. Luo, S. Güven, S. Tasoglu, A. V. Ganesan, A. Weng, U. Demirci, *Adv. Mater.* **2014**, *26*, 5936; d) V. Malkoc, D. Gallego-Perez, T. Nelson, J. J. Lannutti, D. J. Hansford, *J. Micromech. Microeng.* **2015**, *25*, 125001; e) C. Iliescu, G. Xu, W. H. Tong, F. Yu, C. M. B lan, G. Tresset, H. Yu, *Microfluid. Nanofluid.* **2015**, *19*, 363; f) H. Xin, Y. Li, B. Li, *Adv. Funct. Mater.* **2015**, *25*, 2816; g) C. A. DeForest, D. A. Tirrell, *Nat. Mater.* **2015**, *14*, 9.
[9] a) H. Onoe, T. Okitsu, A. Itou, M. Kato-Negishi, R. Gojo, D. Kiriya, K. Sato, S. Miura, S. Iwanaga, K. Kuribayashi-Shigetomi, *Nat. Mater.* **2013**, *12*, 584; b) E. Kang, G. S. Jeong, Y. Y. Choi, K. H. Lee, A. Khademhosseini, S.-H. Lee, *Nat. Mater.* **2011**, *10*, 877.
[10] a) X. Ding, P. Li, S.-C. S. Lin, Z. S. Stratton, N. Nama, F. Guo, D. Slotcavage, X. Mao, J. Shi, F. Costanzo, T. J. Huang, *Lab Chip* **2013**, *13*, 3626; b) S.-C. S. Lin, X. Mao, T. J. Huang, *Lab Chip* **2012**, *12*, 2766.
[11] a) Y. Chen, S. Li, Y. Gu, P. Li, X. Ding, L. Wang, J. P. McCoy, S. J. Levine, T. J. Huang, *Lab Chip* **2014**, *14*, 924; b) J. Shi, D. Ahmed, X. Mao, S.-C. S. Lin, A. Lawit, T. J. Huang, *Lab Chip* **2009**, *9*, 2890; c) F. Guo, Y. Xie, S. Li, J. Lata, L. Ren, Z. Mao, B. Ren, M. Wu, A. Ozcelik, T. J. Huang, *Lab Chip* **2015**, *15*, 4517; d) F. Guo, Z. Mao, Y. Chen, Z. Xie, J. P. Lata, P. Li, L. Ren, J. Liu, J. Yang, M. Dao, *Proc. Natl. Acad. Sci. USA* **2016**, *113*, 6; e) F. Guo, P. Li, J. B. French, Z. Mao, H. Zhao, S. Li, N. Nama, J. R. Fick, S. J. Benkovic, T. J. Huang, *Proc. Natl. Acad. Sci. USA* **2015**, *112*, 43.
[12] W. Pawlina, M. W. Ross, G. I. Kaye, *Histology: A Text and Atlas*, Fourth, Lippincott Williams and Wilkins, Maryland, USA **2003**.
[13] M. Akbari, A. Tamayol, N. Annabi, D. Juncker, A. Khademhosseini, **2014**, Royal Society of Chemistry, Cambridge, England, *Microfluidics for Medical Applications*.
[14] a) R. L. Heise, B. A. Blakeney, R. A. Pouliot, in *Advanced Polymers in Medicine*, Springer, **2015**, 177, Switzerland; b) K. T. Nguyen, J. L. West, *Biomaterials* **2002**, *23*, 4307; c) N. E. Fedorovich, M. H. Oudshoorn, D. van Geemen, W. E. Hennink, J. Alblas, W. J. Dhert, *Biomaterials* **2009**, *30*, 344.

[15] a) R.-Z. Lin, Y.-C. Chen, R. Moreno-Luna, A. Khademhosseini, J. M. Melero-Martin, *Biomaterials* **2013**, *34*, 6785; b) S. T. Koshy, T. C. Ferrante, S. A. Lewin, D. J. Mooney, *Biomaterials* **2014**, *35*, 2477; c) J. W. Nichol, S. T. Koshy, H. Bae, C. M. Hwang, S. Yamanlar, A. Khademhosseini, *Biomaterials* **2010**, *31*, 5536.
[16] Z. Mao, Y. Xie, F. Guo, L. Ren, P.-H. Huang, Y. Chen, J. Rufo, F. Costanzo, T. J. Huang, *Lab Chip* **2016**, *16*, 515.
[17] M. N. Mikhail, M. R. El-Tantawy, *J. Comput. Appl. Math.* **1993**, *45*, 15.
[18] a) J. L. Ifkovits, J. A. Burdick, *Tissue Eng.* **2007**, *13*, 2369; b) V. Chan, P. Zorlutuna, J. H. Jeong, H. Kong, R. Bashir, *Lab Chip* **2010**, *10*, 2062.
[19] T. Tharmalingam, H. Ghebeh, T. Wuerz, M. Butler, *Mol. Biotechnol.* **2008**, *39*, 167.
[20] S. R. Khetani, S. N. Bhatia, *Nat. Biotechnol.* **2008**, *26*, 120.
[21] F. Guo, W. Zhou, P. Li, Z. Mao, N. H. Yennawar, J. B. French, T. J. Huang, *Small* **2015**, *11*, 2733.